ChemPubSoc Europe

DOI: 10.1002/cbic.201300565

Design, Synthesis, and Biological Evaluation of (*S*)-Valine Thiazole-Derived Cyclic and Noncyclic Peptidomimetic Oligomers as Modulators of Human P-Glycoprotein (ABCB1)

Satyakam Singh,[a] Nagarajan Rajendra Prasad,[b, c] Khyati Kapoor,[b] Eduardo E. Chufan,[b] Bhargav A. Patel,[a] Suresh V. Ambudkar,*[b] and Tanaji T. Talele*[a]

Multidrug resistance caused by ATP binding cassette transporter P-glycoprotein (P-gp) through extrusion of anticancer drugs from the cells is a major cause of failure in cancer chemotherapy. Previously, selenazole-containing cyclic peptides were reported as P-gp inhibitors and were also used for co-crystallization with mouse P-gp, which has 87% homology to human P-gp. It has been reported that human P-gp can simultaneously accommodate two to three moderately sized molecules at the drug binding pocket. Our in silico analysis, based on the homology model of human P-gp, spurred our efforts to investigate the optimal size of (*S*)-valine-derived thiazole units that can be accommodated at the drug binding pocket. Towards this goal, we synthesized varying lengths of linear and cyclic derivatives of (*S*)-valine-derived thiazole units to investigate the optimal size, lipophilicity, and structural form (linear or cyclic) of valine-derived thiazole peptides that can be accommodated in the P-gp binding pocket and affects its activity, previously an unexplored concept. Among these oligomers, lipophilic linear (**13**) and cyclic trimer (**17**) derivatives of QZ59S-*SSS* were found to be the most and equally potent inhibitors of human P-gp (IC_{50} = 1.5 μM). As the cyclic trimer and linear trimer compounds are equipotent, future studies should focus on noncyclic counterparts of cyclic peptides maintaining linear trimer length. A binding model of the linear trimer **13** within the drug binding site on the homology model of human P-gp represents an opportunity for future optimization, specifically replacing valine and thiazole groups in the noncyclic form.

Introduction

P-glycoprotein (P-gp) or multidrug resistance protein 1 (MDR1), encoded by *ABCB*1, is a plasma membrane-bound ATP-binding cassette (ABC) transporter. P-gp catalyzes the ATP-dependent efflux of a highly diverse set of compounds, including amphipathic, neutral, or weakly basic compounds with molecular weights ranging from less than 200 to 2000 Da.[1–3] The 1280-residue human P-gp consists of two transmembrane domains (TMDs), each with six α-helices and two nucleotide-binding domains (NBDs). The drug/substrate binding sites are predicted to be located in the TMDs.[4,5] It has been well established that the drug binding pocket is even capable of binding to two to three molecules simultaneously.[4,6–9] Drug transport by P-gp is driven by hydrolysis of ATP at NBDs. The close conformation of NBDs generated by ATP binding/hydrolysis mediates substrate translocation from the drug binding sites in TMDs, thus triggering release of the substrate to the extracellular face of the membrane.[10,11]

In cancer patients, resistance to chemotherapy is a critical issue and can be due to various mechanisms. Overexpression of multidrug resistance (MDR) proteins such as P-gp is one of the well-studied mechanisms of drug resistance.[12] Upregulation of ABC drug transporters has been demonstrated in a variety of cancer types and has been shown to result in reduced intracellular concentration of chemotherapeutic drugs. P-gp is largely recognized for its role in enabling cancer cells to evade response to treatment through the efflux of chemotherapeutic agents. This multidrug resistance impedes the clinical efficiency of chemotherapy. Therefore, many researchers have been engaged in developing human P-gp inhibitors to reverse the chemotherapeutic drug resistance. As there is no high-resolution crystal structure of human P-gp yet available, a homology model of human P-gp based on the crystal structure of P-gp from mouse[13] serves as a tool for structure-based drug design of P-gp inhibitors. Although various strategies, such as random and focused screening, systematic chemical modifications, and

[a] Dr. S. Singh, B. A. Patel, Dr. T. T. Talele
Department of Pharmaceutical Sciences
College of Pharmacy and Health Sciences, St. John's University
8000 Utopia Parkway, Queens, NY 11439 (USA)
E-mail: talelet@stjohns.edu

[b] Dr. N. R. Prasad, Dr. K. Kapoor, Dr. E. E. Chufan, Dr. S. V. Ambudkar
Laboratory of Cell Biology, Center for Cancer Research
National Cancer Institute, National Institutes of Health
37 Convent Drive, Bethesda, Maryland 20892-4256 (USA)
E-mail: ambudkar@mail.nih.gov

[c] Dr. N. R. Prasad
Current address:
Department of Biochemistry and Biotechnology, Annamalai University
Annamalai Nagar, Annamalai 608002, Tamilnadu (India)

Supporting information for this article is available on the WWW under http://dx.doi.org/10.1002/cbic.201300565.

combinatorial chemistry have been pursued thus far to develop the first three generations of P-gp inhibitors, their toxicity and drug interaction profiles are still undesirable. Therefore, new strategies leading to the development of fourth generation P-gp inhibitors (isolation of natural products or chemically modified natural product analogues) with high P-gp selectivity and potency seems to be a novel approach.[14]

Analysis of QZ59-selenazole cyclic peptides (QZ59Se-*SSS* and QZ59Se-*RRR*)[5] within the drug binding cavity of a human P-gp homology model (built previously by using mouse P-gp)[13] led to the following observations: 1) two copies of QZ59Se-*SSS* were found at the QZ59Se-*SSS* binding site[5] (Figure 1); moreover, it has been reported that human P-gp can simultaneously accommodate two to three molecules at the drug binding transmembrane domain.[4,6–9] 2) P-gp can distinguish between the stereoisomers of cyclic peptides such that QZ59Se-*SSS* forms extensive hydrophobic contacts with the hydrophobic residues of the drug binding site and is four times more potent than the corresponding QZ59Se-*RRR* isomer. Therefore, in our design strategy described below, we chose to maintain *S* stereochemistry at all chiral centers. 3) Comparison of inhibitory activity of QZ59S-*SSS* for Chinese hamster or mouse P-gp ($IC_{50} = 2.7\ \mu M$)[15] with that of potent inhibitor valspodar[16] suggests a role of macrocyclic peptidic nature of valspodar for its high potency as compared to QZ59Se-*SSS* (Figure 1). During ongoing phase III clinical trials, valspodar has shown very restricted oral bioavailability which, along with its efficacy and safety concerns, further suggested the need for optimization.[17]

Unlike valspodar and cyclosporine A, both of which are macrocyclic undecamer peptides, our peptidomimetic oligomers incorporate insertion of thiazole ring between the Cα-carbon and carbonyl carbon, thus making them non-natural peptides that could be potentially devoid of immunosuppressant activi-

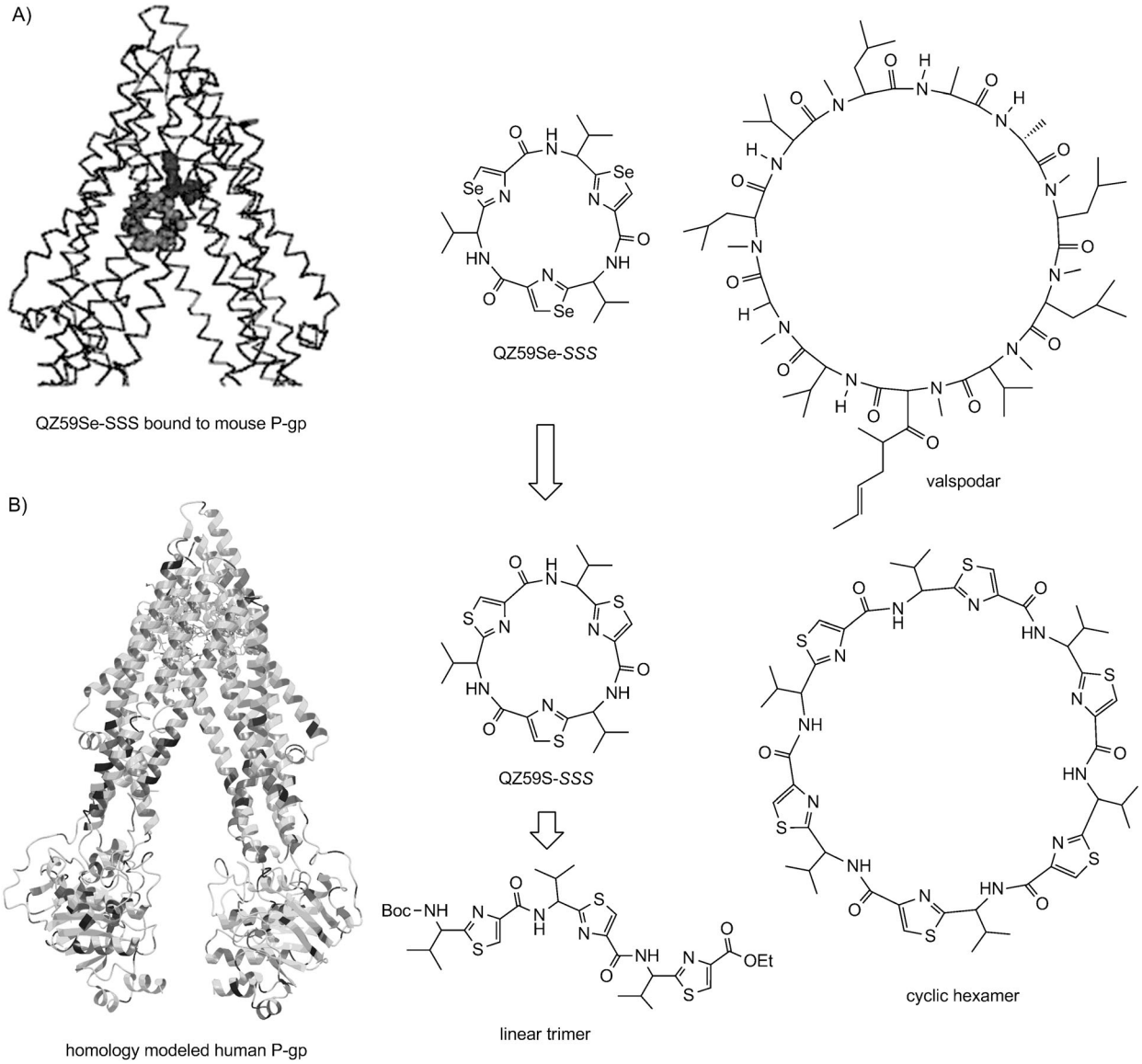

Figure 1. Design strategy: A) schematic structure of mouse P-gp crystal structure bound to QZ59Se-*SSS*[5] and chemical structures of QZ59Se-*SSS* and valspodar; B) human P-gp homology model generated from mouse P-gp (PDB ID: 3G60), cyclic trimer QZ59S-*SSS* along with its structural (shape) variant linear trimer and the cyclic hexamer.

ty as well as resistant to hydrolytic cleavage by proteases. The constrained five-membered thiazole ring imposes conformational restrictions that lead to entropically favorable binding at the drug binding site of P-gp. With this backdrop, herein we report the effect of structural form, length, and flexibility of the designed (*S*)-valine thiazole-derived peptidomimetic oligomers on human P-gp function.

The co-crystal structure of QZ59Se-*SSS* and mouse P-gp has been previously reported.[5] The sulfur analogue was also shown to have an IC_{50} value of 2.7 μM against mouse P-gp;[15] however, the study reported here illustrates the inhibitory activity of QZ59S-*SSS* against human P-gp. Replacement of selenium with sulfur could be an effective strategy for designing natural product analogues, which are better tolerated by human cells. Thiazole structures are abundant in natural products and have direct applications in drug discovery.[18] Furthermore, we performed docking experiments on these analogues at all of the possible binding sites of homology modeled human P-gp.

Results and Discussion

Chemistry

The thiazole derivatives were synthesized with diminutive variations in the procedures reported by Bertram et al. and as shown in Schemes 1 to 6.[19,20] Compounds with one thiazole unit, both linear and cyclic, are referred to as monomeric derivatives, those with two thiazole units are called dimeric, and so forth (trimeric, tetrameric, and hexameric). Scheme 1 shows the synthesis of monomeric derivatives, starting with commercially available *N*-Boc-(*S*)-valine (**1**), which was converted to amide **2** by a general mixed anhydride/aqueous ammonia method in quantitative yield (Scheme 1). Amide **2** was then transformed to thioamide **3** by a Holpfazel–Hantzsch procedure[21] using Lawesson's reagent in tetrahydrofuran (THF).[22,23] Compound **5** was synthesized by a modified Hantzsch method.[24,25] This procedure involves a reaction between compound **3** and ethyl bromopyruvate to give the cyclocondensed intermediate 4,5-dihydrothiazole **4**, which, upon treatment with trifluoroacetic anhydride (TFAA), furnished aromatized thiazole product **5** in low yields.[21] Here, highly acidic reaction conditions in the later step present a possibility for *N*-trifluoroacetylation of amide NH. For this reason, the crude product obtained was further treated with freshly prepared sodium ethoxide in ethanol to produce the desired product **5** in appreciable yields without affecting the stereocenter adjacent to the 2-position of the thiazole ring. Next, saponification of compound **5** with sodium hydroxide produced the monomeric acid (**6**), and deprotection of the Boc-NH in compound **5** by using trifluoroacetic acid (TFA) produced the monomeric amine TFA salt (**7**). Further, Boc-deprotection of carboxylic acid derivative **6** yielded zwitterion product **8** (Scheme 1).

Next, through quick initial experiments, we optimized the coupling of valine-derived monomeric thiazole acid (**6**) through activation with BOP (benzotriazol-1-yl-oxy)-tris(dimethylamino)phosphonium hexafluorophosphate reagent), HOBt, and DIEA in CH_2Cl_2/DMF (4:1) with an excess of monomer thiazole amine (**7**) to produce the required dimer (**9**) in moderate yield, as shown in Scheme 2. This may be attributed to the sterically demanding isopropyl group adjacent to the amine functionality.[26,27] Compounds **10** and **11** were synthesized by basic and acidic hydrolysis of dimer **9**, respectively. Further, deprotected compound **12** was made by treating dimer acid **10** with TFA in DCM (Scheme 2). The synthetic route to trimer derivatives is portrayed in Scheme 3. Monomeric amine **7** and dimeric acid **10** were coupled by using the BOP-HOBt method to obtain the desired linear trimer (**13**). Compound **13** was hydrolyzed by sodium hydroxide and TFA, respectively, to give trimeric acid **14** and trimeric amine **15**. Acid **14** was again treated with TFA in DCM to obtain intermediate trimeric zwitterion **16**, which was carried forward without further purification. Intermediate **16** was cyclized in the presence of pentafluorophenyl diphenylphosphinate (FDPP), anhydrous $ZnCl_2$, and DIEA in CH_2Cl_2/DMF (4:1) to provide the target cyclic trimer (**17**; QZ59S-*SSS*).[28] Alternatively, cyclic trimer **17** was prepared by coupling and subsequent cyclization of three molecules of monomer zwitterion compound **8** according to the above mentioned procedure. The above compounds were found to be optically pure ($ee \geq 95\%$), based on analysis by chiral HPLC (single peak when using acetonitrile/water/TFA 85:15:0.1). After exploring a number of different conditions to prepare linear peptides, we found that coupling re-

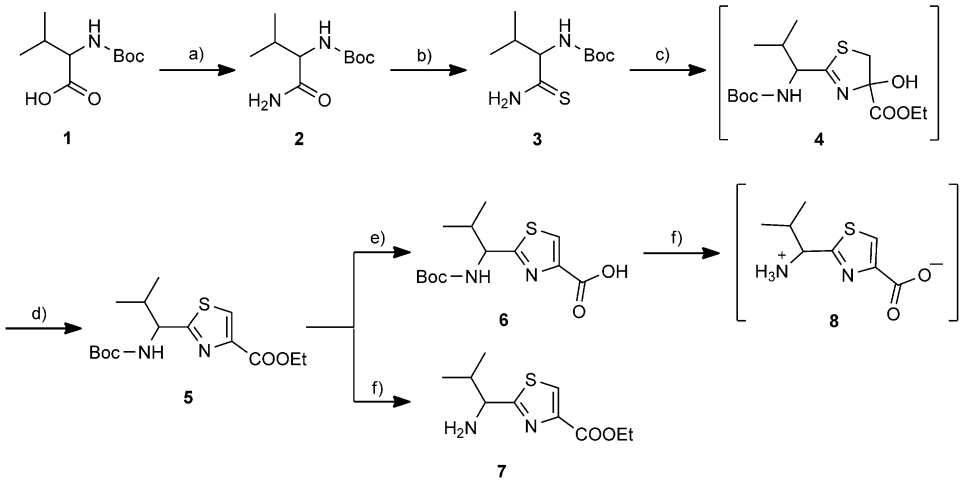

Scheme 1. Reagents and conditions: a) i: isobutyl chloroformate, *N*-methyl morpholine, THF, −20 °C, 4 h; ii: 30% NH_4OH in excess, −20 °C to RT, 4 h; b) Lawesson's reagent, THF, 50 °C, 16 h; c) ethyl bromopyruvate, $KHCO_3$, DME, −15 °C to RT, 12 h; d) i: TFAA, 2,6-lutidine, DME, −15 °C to RT, 15 h; ii: NaOEt, EtOH, −15 °C to RT, 6 h; e) NaOH, THF/MeOH/H_2O (10:2:3), RT, 4 h; f) TFA, CH_2Cl_2, RT, 12 h.

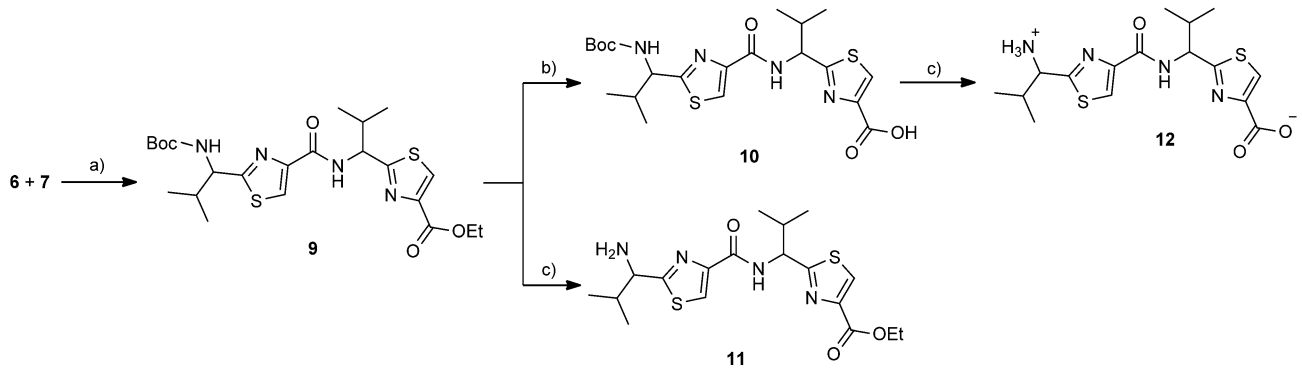

Scheme 2. Reagents and conditions: a) BOP, HOBt, DIEA, CH_2Cl_2/DMF (4:1), RT, 18 h; b) NaOH, THF/MeOH/H_2O (10:2:3), RT, 4 h; c) TFA, CH_2Cl_2, RT, 12 h.

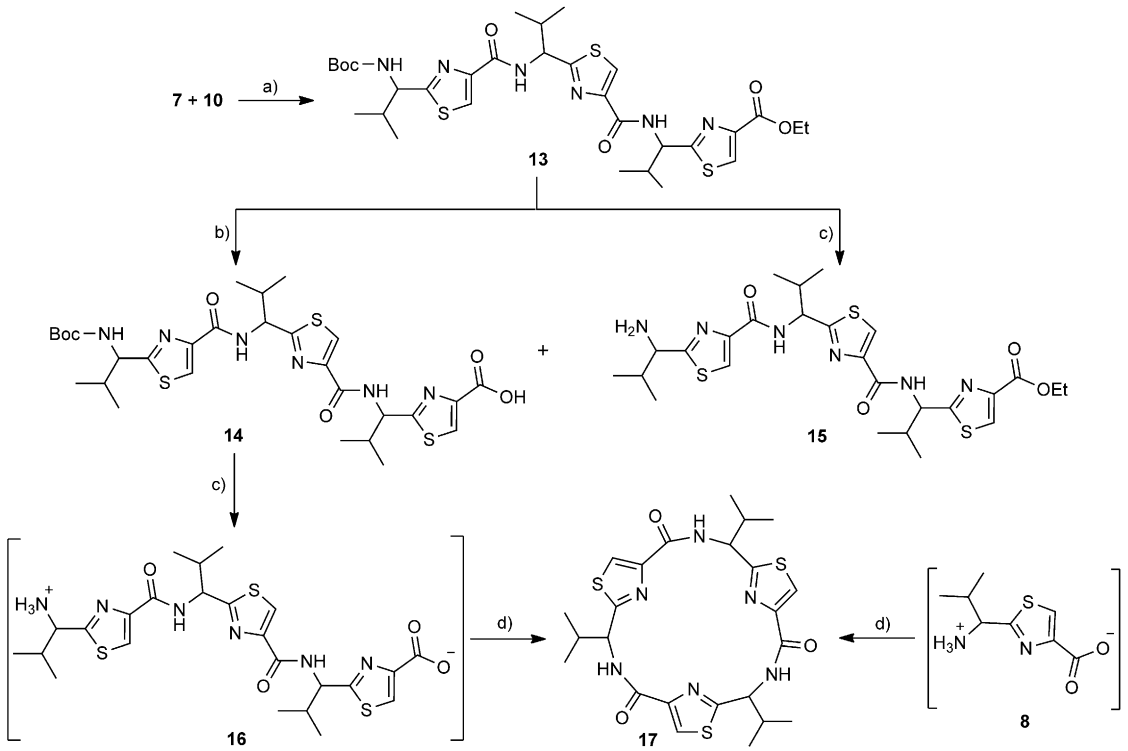

Scheme 3. Reagents and conditions: a) BOP, HOBt, DIEA, CH_2Cl_2/DMF (4:1), RT, 18 h; b) NaOH, THF/MeOH/H_2O (10:2:3), RT, 4 h; c) TFA, CH_2Cl_2, RT, 12 h; d) FDPP, DIEA, anhydrous $ZnCl_2$, CH_2Cl_2/DMF (4:1), RT, 5 d.

actions of thiazole acid in the presence of 1.5 equiv of BOP, 1.5 equiv of HOBt, and 1.5 equiv of *N*,*N*-diisopropylethylamine (DIEA), with valine-derived thiazole amine TFA salt in excess amounts (1.3–1.5 equiv) in CH_2Cl_2/DMF (4:1) worked satisfactorily. Linear derivatives of tetramer **18** and hexamer **19** were prepared from corresponding thiazole starting materials (Scheme 4). Compound **18** was prepared by coupling **10** and **11**; linear hexamer **19** was synthesized beginning from **14** and **15**. The cyclic tetramer (**20**) and cyclic hexamer (**21**) were synthesized starting from dimer zwitterion (**12**), giving both products in one step (Scheme 5). The tetramer and hexamer derivatives were produced in very low yields (Schemes 4 and 5); therefore, the desired products were purified and characterized by means of preparative HPLC with subsequent electron spray ionization-mass spectrometry (ESI-MS) analysis. In our further investigation, the carboxy terminus of valine-derived bis-thiazole acid (**10**) was coupled with commercially available arylalkyl amines **22a** and **23a** by using coupling reagents HCTU, HOBt, and DIEA in DMA to obtain compounds **22** and **23** in moderate yield, as shown in Scheme 6. The activity of the synthesized analogues was assessed for P-gp modulation by using calcein-AM and BODIPY-FL-Prazosin efflux assays, inhibition of photolabeling of P-gp with [^{125}I]iodoarylazidoprazosin ([^{125}I]IAAP), and an ATPase activity assay.

Structure–activity relationships

The thiazole-containing peptides were studied for their modulatory effects on the transport function of human P-gp. Herein, we wanted to investigate the optimal size, lipophilicity, and

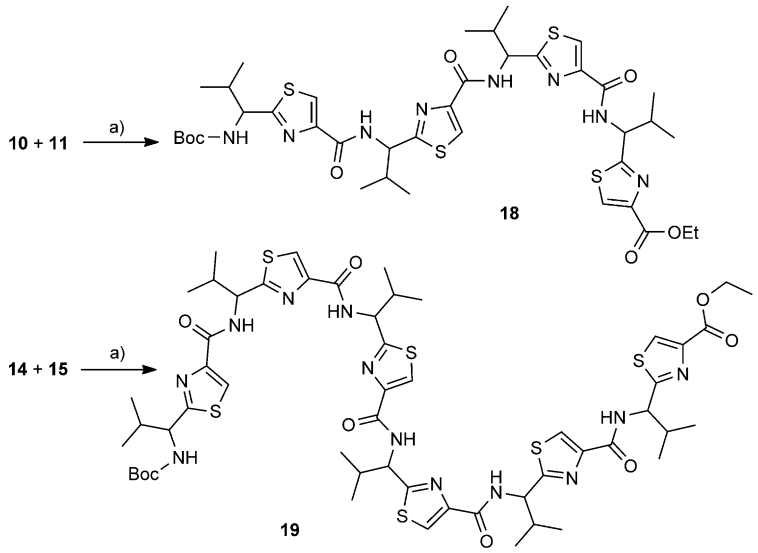

Scheme 4. Reagents and conditions: a) BOP, HOBt, DIEA, CH_2Cl_2/DMF (4:1), RT, 18 h.

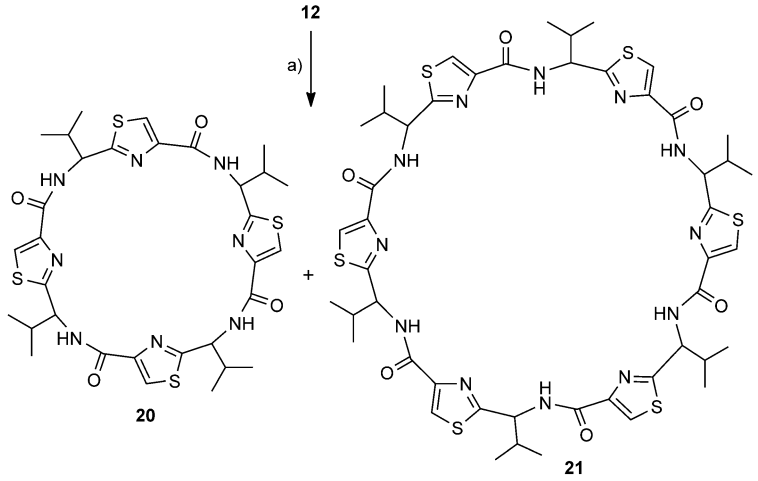

Scheme 5. Reagents and conditions: a) FDPP, DIEA, CH_2Cl_2/DMF (4:1), RT, 5 d.

structural form (linear and cyclic) of these peptides that can be accommodated well in the P-gp drug binding pocket and affect P-gp activity.

The synthesized (*S*)-valine-derived thiazole products (**5**–**15**, **17**–**23**) were evaluated for their effect on human P-gp activity utilizing multiple assays. Table 1 represents the percent inhibition values for all thiazole derivatives obtained from calcein-AM and BODIPY-FL-Prazosin efflux assays in HeLa cells expressing human P-gp. In Table 1, inhibition of P-gp transport activity by the synthesized compounds was expressed as relative to the percent inhibition caused by 1 μM tariquidar, a known third generation P-gp inhibitor.[29–31] All the synthesized derivatives were tested for their effects on photoaffinity labeling of P-gp with [^{125}I]IAAP, which is a transport substrate for P-gp; results are given in Table 2. For comparison of inhibitory potency of our derivatives, we used tariquidar as a standard inhibitor of photolabeling of P-gp [^{125}I]IAAP, with 5 μM tariquidar giving complete (100%) inhibition (see Table 2).

The monomeric compounds comprising a single thiazole unit (**5**–**8**) were devoid of P-gp inhibitory activity, as indicated by data obtained from the efflux assays (<5–10% inhibition). These results were also corroborated by [^{125}I]IAAP % inhibition. Ineffective inhibition of P-gp efflux function by monomers **5**–**8** might possibly be due to their smaller size and limited hydrophobic surface area. In this regard, increasing the number of thiazole units to two in compound **5**, thus resulting in compound **9**, was found to result in substantial improvement in P-gp inhibition. Dimeric compound **9** inhibited calcein-AM efflux by 55% and [^{125}I]IAAP labeling by 87%, as compared to <5% and 20%, respectively, for monomeric compound **5**. In contrast, BODIPY-FL-Prazosin efflux analysis (20% inhibition) showed modest improvement for compound **9**. However, compounds **10** and **12**, the corresponding acid and zwitterion derivatives, respectively, of **9**, exhibited complete loss in inhibitory activity (<5% calcein-AM efflux inhibition; 12% and 9% BODIPY-Prazosin efflux inhibition, respectively). On the other hand, amine **11** maintained similar inhibition potency to that of compound **9** (55% calcein-AM efflux inhibition and 13% BODIPY-FL-Prazosin efflux inhibition). Among the dimers, a free carboxy group proved unfavorable, which might be due to poor cell penetration. However, dually protected dimer **9**, as well as its Boc-hydrolyzed analogue **11**, both showed identical inhibition of P-gp efflux function as compared to acid **10** and zwitterion **12**. The [^{125}I]IAAP labeling inhibition results for these dimeric derivatives (**10**, <10%; **11**, 87%; **12**, 23%) corresponded to data from the efflux assays. These results suggest that the free acid group is not accepted; however, the free amino group is rather well tolerated in the P-gp binding pocket, as this moiety is frequently seen in P-gp modulators.[32] Next, further increasing the length to a tripeptide, compound **13** showed impressive activity with 98% inhibition of calcein-AM efflux by P-gp, along with 75% inhibition of BODIPY-FL-Prazosin transport. The dose–response curve for this analogue against calcein-AM efflux function revealed an IC_{50} of 1.5 μM. In affirmation of this activity, [^{125}I]IAAP labeling was inhibited by a significant extent (91%). In addition to this substantial enhancement, deprotection of compound **13** was effected at both ends. As observed for compound **10**, acid **14** was devoid of calcein-AM or BODIPY-FL-Prazosin efflux inhibition potential (<10%) but showed moderate (60%) inhibition of [^{125}I]IAAP labeling of P-gp. From these results, it is evident that larger molecular size, coupled with extended hydrophobic surface area and lipophilic characteristics are the key features contributing towards increased inhibition of P-gp efflux function. The increase in the [^{125}I]IAAP labeling inhibition by compound **14** might be due to an increase in the hydrophobic segment as compared to dimer acid **10**, and lack of transport

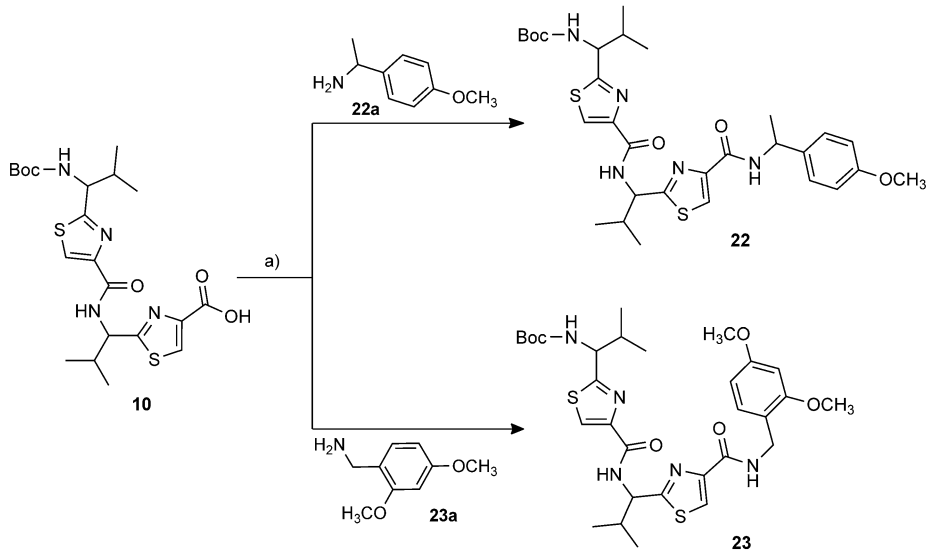

Scheme 6. Reagents and conditions: a) HCTU, HOBt, DIEA, DMA, RT, 18 h.

function inhibitory activity could be attributed to the fact that these cell-based assays require compounds to permeate the lipophilic cell bilayer. Amine derivative **15** showed moderate inhibitory activity of 55 and 67% for transport, yet still maintained 91% inhibition of [^{125}I]IAAP labeling. Subsequently, trimer **13** was cyclized to obtain compound **17** (i.e., QZ59S-*SSS*) and evaluated against human P-gp efflux function. The observed results suggest that the linear and cyclic forms of the tripeptide structure are equipotent, based on the inhibition of calcein-AM efflux (inhibition = 97%, IC_{50} = 1.5 μM), BODIPY-FL-Prazosin assay (89%), and the [^{125}I]IAAP labeling assay (87%). The results obtained from trimeric analogues further reinforce the notion that increased molecular size and hydrophobicity contribute towards inhibition of P-gp efflux function. As increasing molecular size and hydrophobicity proved beneficial to inhibit P-gp efflux activity, we decided to hereafter synthe-

Table 1. Effect of (*S*)-valine-based thiazole derivatives on the transport function of P-gp in HeLa cells.

Compound	Common name	Tested conc. [μM]	Inhibition of efflux[a] [%] Calcein-AM	BODIPY-Prazosin
5	monomer	20	< 5	10
6	monomer acid	20	< 5	10
7	monomer amine	20	< 5	< 5
8	monomer zwitterion	20	< 5	n.d.[c]
9	dimer	20	55	20
10	dimer acid	20	< 5	12
11	dimer amine	20	55	13
12	dimer zwitterions	20	< 5	9
13	linear trimer	10	98[b]	75
14	trimer acid	10	< 5	10
15	trimer amine	10	55	67
17	cyclic trimer (QZ59S-*SSS*)	10	97[b]	89
18	linear tetramer	10	59	81
19	linear hexamer	10	< 5	12
20	cyclic tetramer	10	62	79
21	cyclic hexamer	10	< 5	15
22	*R*-1-(4-methoxy-phenyl)-ethyl dimer acid	10	97[b]	88
23	2,4-dimethoxy benzyl amine dimer acid	10	91[b]	87

[a] BacMam-P-gp virus-transduced HeLa cells were incubated with 0.5 μM calcein-AM for 10 min or BODIPY-FL-Prazosin for 45 min at 37 °C in the dark in the presence and absence of 10 μM (*S*)-valine-based thiazole derivatives. Cells were washed once with IMDM medium and data acquired in FL-1 channel in a flow cytometer. The percentage of transport inhibition was derived by taking the level of inhibition obtained with a known P-gp inhibitor, tariquidar, at 1 μM equal to 100%, and the values shown are an average of two independent experiments done in triplicate. [b] The IC_{50} values of inhibition of calcein-AM efflux for selected compounds: **13** (linear trimer) = 1.5 μM; **17** (cyclic trimer) = 1.5 μM; **22** (*R*-1-(4-methoxyphenyl)ethyl dimer acid) = 2.0 μM; and **23** (2,4-dimethoxybenzyl amine dimer acid) = 2.0 μM. These values were determined by taking the average of at least two independent experiments done in triplicate. [c] Not determined.

Table 2. Effect of (*S*)-valine-based thiazole derivatives on photolabeling of P-glycoprotein with [^{125}I]IAAP.

Compound	Common name	Tested conc. [μM]	[^{125}I]IAAP inhibition[a] [%]
5	monomer	20	20
6	monomer acid	20	< 10
7	monomer amine	20	< 10
8	monomer zwitterion	20	< 10
9	dimer	20	87
10	dimer acid	20	< 10
11	dimer amine	20	87
12	dimer zwitterion	20	23
13	linear trimer	10	91
14	trimer acid	10	60
15	trimer amine	10	91
17	cyclic trimer (QZ59S-*SSS*)	10	87
18	linear tetramer	10	99
19	linear hexamer	10	94
20	cyclic tetramer	10	95
21	cyclic hexamer	10	91
22	*R*-1-(4-methoxy-phenyl)-ethyl dimer acid	10	100
23	2,4-dimethoxybenzyl-amine dimer acid	10	95

[a] Crude membranes (50–75 μg protein) from P-gp-expressing High-Five insect cells were incubated in the presence and absence of 10 μM thiazole derivatives in 50 mM Tris·HCl (pH 7.5) and 4–6 nM [^{125}I]IAAP (2200 Ci mmol^{-1}). The samples were then photo-crosslinked by exposure to 366 nm UV light for 10 min, and incorporation of [^{125}I]IAAP was determined on a phosphorimager as described previously.[45] The positive control (5 μM tariquidar) inhibited IAAP incorporation into P-gp by 100%. The results are given as percent inhibition of [^{125}I]IAAP incorporation into P-gp by taking the average of two independent experiments.

size only the lipophilic linear structure protected at both ends and the cyclic form for higher analogues such as tetramers and hexamers. In this direction, four units of thiazole-containing linear tetramer **18** were tested to find that the cell-based inhibitory activity (59 and 81%), decreased by 1.6-fold as compared to that of homologue **13** despite an increase in [^{125}I]IAAP labeling inhibition (99%). Surprisingly, the linear hexamer (**19**) lacked any significant P-gp efflux inhibitory activity (5 and 12%) in transport assays. Additionally, cyclic tetramer **20**, which showed moderate inhibition of efflux transport (62 and 79%) demonstrated appreciable inhibition of [^{125}I]IAAP labeling (95%) of P-gp. Similar to its linear analogue, cyclic hexamer (**21**) also proved to be ineffective in transport assays (<5 and 15%). It was interesting to note that linear and cyclic hexamers (**19** and **21**) did not inhibit calcein-AM or BODIPY-FL-Prazosin transport significantly, although these derivatives significantly inhibited photoaffinity labeling of [^{125}I]IAAP (94% for **19** and 91% for **21**). This suggests that the hexameric compounds interact with P-gp, contrary to the transport assay results. These discrepancies may be ascribed to decreased ability of the higher analogues of the trimeric compounds to cross the cell membrane in short-term transport assays.

Functionally, P-gp possesses ATPase activity that is stimulated by many substrates.[33,34] ATPase stimulation activity for selected derivatives (**13**–**15**, **17**–**23**) was determined by using membranes of P-gp-expressing High-Five insect cells (Table 3). Here as well, the linear (**13**, fold stimulation = 2.80) and the cyclic (**17**, fold stimulation = 2.81) trimer analogues were found to stimulate the ATPase activity equivalently. Corresponding to the above transport assays, the trimeric acid (**14**, fold stimulation = 1.47) was less effective, whereas an increase in ATPase activity by the amine derivative (**15**, fold stimulation = 2.16) was comparable to that of compound **13**. For the higher analogues, the ATPase activity fold stimulation data was consistent with results from the labeling assay; this suggests that these compounds interact with P-gp. For comparison, we used the well-established substrate verapamil,[35] which is also a good stimulator of ATPase activity,[33,34] and found that 50 μM verapamil gave 2.5-fold stimulation of P-gp ATPase activity (see Table 3). Nonetheless, the results presented here suggest that the ability to cross the cell membrane decreases with an increase in the size of the molecule above that of the trimer-length structures. Furthermore, to understand the binding mechanism of oligomers to the drug binding pocket of the homology model of human P-gp[13,36] at molecular level, we performed glide docking using ABCB1-QZ59Se-*RRR* (site 1), ABCB1-QZ59Se-*SSS* (site 2), ABCB1-verapamil (site 3), a site common to the above three sites (site 4)[5] and the ATP binding site, following the protocol mentioned in our previous studies.[13,36] Binding energy data for the docked poses of oligomers were compared at all sites, and the QZ59Se-*RRR* binding site of P-gp (site 1) was found to be the most favorable site for binding of linear trimer analogue **13**, which was also supported by the photoaffinity labeling assay with substrate [^{125}I]IAAP (Table 2).

Table 3. Effect of selected thiazole derivatives on vanadate-sensitive ATPase activity of P-glycoprotein.

Compound	ATPase activity [nmol P_i min^{-1} per mg protein][a]	Fold stimulation
13	78.00	2.80
14	41.40	1.47
15	60.70	2.16
17	78.75	2.81
18	83.70	2.98
19	54.30	1.93
20	42.15	1.50
21	77.20	2.75
22	89.40	3.31
23	92.30	3.42

[a] Crude membranes (100 μg protein mL^{-1}) from P-gp expressing High-Five cells were incubated at 37 °C with 2.5 μM of selected derivatives in the presence and absence of 0.3 mM sodium orthovanadate in ATPase assay buffer for 5 min, then the vanadate-sensitive ATPase activity of P-gp was determined as described.[44] Vanadate-sensitive ATPase activity was calculated as nmol P_i per min per mg protein and expressed as fold stimulation with respect to basal ATPase activity (in the presence of DMSO solvent) taken as 1.0. For the same membranes, 50 μM verapamil stimulated the ATPase activity of P-gp by 2.5-fold (70 nmol P_i min^{-1} mg^{-1} protein). The values are an average of two independent experiments.

The flow cytometer-based transport assay was used with fluorescent substrates to test the potency of synthesized derivatives. Figure 2A shows a typical histogram of the effect of selected compounds on calcein-AM efflux by P-gp. It is clear from the Figure that linear trimer **13** is as effective in its cyclic form (**17**) at 5 μM, whereas the dimer (**9**) is moderately and the monomer (**5**) is least effective. For comparison, inhibition of calcein-AM efflux with 1 μM tariquidar is also shown in Figure 2A (tainted filled trace). Figure 2B depicts the concentration-dependent effect of these three compounds and, from the inhibition curves, IC_{50} values (concentrations required for 50% inhibition) were determined. The IC_{50} values for the linear (**13**) and cyclic (**17**) trimers were similar (1.5 μM; see Table 1), whereas for the dimer (**9**), it was much higher (20 μM; Figure 2B).

The data obtained thus far suggests that trimeric length, both for linear and cyclic compounds, was optimal for blocking P-gp efflux activity. To this end, we synthesized two derivatives (**22** and **23**) of dimer acid **10** by coupling with the corresponding methoxy-substituted arylalkyl amines to mimic the trimer length. A critical role of methoxy-substituted arylalkyl amines in tariquidar and elacridar towards P-gp inhibition prompted us to choose these pharmacophores. Further, we chose a dimeric acid, in spite of its inactivity, because protected dimer **9** was found to be active, thus indicating a possible role for the carboxy terminal extension in enhanced binding. Also, we wanted to limit the size of the resulting chain to a trimer because analogues higher than a trimer proved ineffective. Indeed, these compounds showed significant efflux inhibition of both calcein-AM and BODIPY-FL-Prazosin (**22**, inhibition = 97 and 88%; **23**, inhibition = 91 and 87%) as well as [^{125}I]IAAP labeling of P-gp (**22**, inhibition = 100%; **23**, inhibition = 95%). The IC_{50} values for inhibition of calcein-AM efflux for both **22** and **23** were found to be 2.0 μM (see Table 1). Both **22** and **23** also stimulated ATPase activity of P-gp by 3.31- and 3.42-fold, respectively.

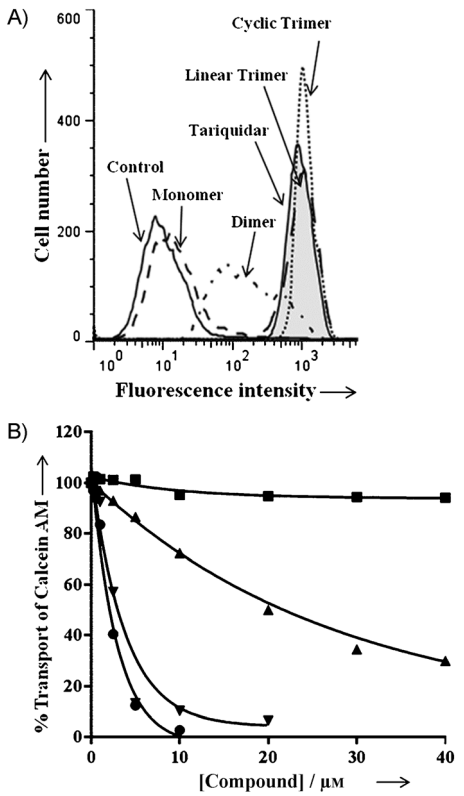

Figure 2. Inhibition of P-gp-mediated calcein-AM transport by various derivatives. HeLa cells transduced with wild-type P-gp BacMam virus were evaluated for transport function by using calcein-AM (0.5 μM) as described in the Experimental Section. A) Reversal of calcein-AM transport was carried out in the presence of solvent DMSO (control, solid line), or in the presence of various synthesized derivatives at 5 μM. The reversal by monomer **5** (dashed line), dimer **9** (complex line), linear trimer **13** (long dashed line), and cyclic trimer **17** (QZ59S-*SSS*; dotted line) were compared with tariquidar (1 μM), which is a known inhibitor of P-gp (tinted filled trace). B) BacMam P-gp-transduced HeLa cells were assayed for calcein-AM transport in the presence of increasing concentrations of monomer **5** (■), dimer **9** (▲), linear trimer **13** (▼), and cyclic trimer **17** (QZ59S-*SSS*; ●). Transport in the absence of these compounds was taken as 100%. The results are represented as an average of two independent experiments. The IC_{50} value for the dimer (**9**) was 20 μM, and the value for both the linear trimer (**13**) and the cyclic trimer (**17**) was 1.5 μM.

In general, log*P* values of resulting compounds could have a major role in the activity of compounds, as observed in various QSAR analyses of P-gp inhibitors.[37–39] It is evident that lipophilicity contributes significantly to high P-gp inhibitory activity. These studies have also described that molecules with log*P* values between 3 and 6 have been shown to exhibit higher mean efflux ratios.[37–39] Interestingly, the QikProp-derived *clog P* values of potent trimer analogues (**13**, **17**, **22**, and **23**) were found to be within the range of 3 and 6. However, the higher oligomers, namely tetramer and hexamer derivatives **18**–**21** were in a higher range of *clog P* values (6–9), which could have been a possible barrier for the inhibitory activity of P-gp, whereas inactive zwitterion compounds were found to have negative *clog P* values. This is also evident from the graphs illustrated in Figure S1 A–D (see the Supporting Information). There is a clear correlation between size and potency of derivatives until ~850 Da for inhibition of transport, but for inhibition of [^{125}I]IAAP incorporation and stimulation of ATPase activity, which are not transport assays, the same does not hold true.

Molecular docking

The binding model of linear trimer **13** (labeled as X1) is shown in Figure 3 A and B. The Boc *tert*-butyl group is involved in hydrophobic contacts with the side chains of residues L304 and M986, whereas the carbamate group of Boc enters into electrostatic interactions with Q725 (–NH···O(H_2N)C-Q725, 3.2 Å) and Q990 (–C(H_3C)$_3$–O···H_2N(O)C-Q990, 2.8 Å). The thiazole ring nitrogen atom next to the carbamate group is involved in electrostatic interactions with Q725 (N···H_2N(O)C-Q725, 2.2 Å). Further, the carbonyl oxygen atom attached to the same thiazole ring was shown to have a critical hydrogen bonding interaction with Y307 (–CO···HO-Y307, 2.0 Å). The thiazole rings and isopropyl groups are responsible for the significant interactions with M69, F72, F336, F343, F728, A729, F732, F957, F978 and V982. The ethyl group of the ester functionality is located in the vicinity of hydrophobic residues L65, M68 and M949. The thiazole ring nitrogen atom near the ester group is shown to have another hydrogen bonding interaction with Y953 (–CO··· HO-Y953, 2.4 Å).

Among these residues, Y307, Q725, F728, and V982 might have a significant role in interactions, as these residues were found to be involved with most of the ligands during docking to different drug binding sites of human P-gp. These residues were also shown to be critical based on labeling with methanethiosulfonate (MTS)-verapamil.[40]

Conclusions

We synthesized a series of (*S*)-valine-derived thiazole-containing cyclic and noncyclic peptidomimetic oligomers to identify the optimal structural requirements for potent inhibition of human P-gp. Based on a set of 17 compounds from monomer to hexamer, it was revealed that linear (**13**) and cyclic (**17**) trimer oligomers of (*S*)-valine-derived thiazole units were found to be the most potent inhibitors of human P-gp (IC_{50} = 1.5 μM), with potency comparable to third generation inhibitors (e.g., tariquidar) of this transporter. In addition, our analysis also indicated the importance of the molecular size, lipophilicity, and hydrophobic contact surface area of the synthesized compounds. As the cyclic trimer and linear trimer were equipotent, future studies should focus on noncyclic versions of various known cyclic peptides. The binding model of compound **13** within the drug binding site on the homology model of human P-gp represents an opportunity for future optimization with linear trimers based on the present interactions. Two representative dimer analogues (**22** and **23**) were also synthesized to verify the hypothesis that maintaining a length up to trimer improves inhibition of P-gp efflux function. Indeed, **22** and **23** were shown to have significant inhibitory capacity on human P-gp efflux transport. Therefore, future SAR will be mainly devoted to dimer derivatives modified to mimic a trimer length to obtain highly active inhibitors specific for human P-gp.

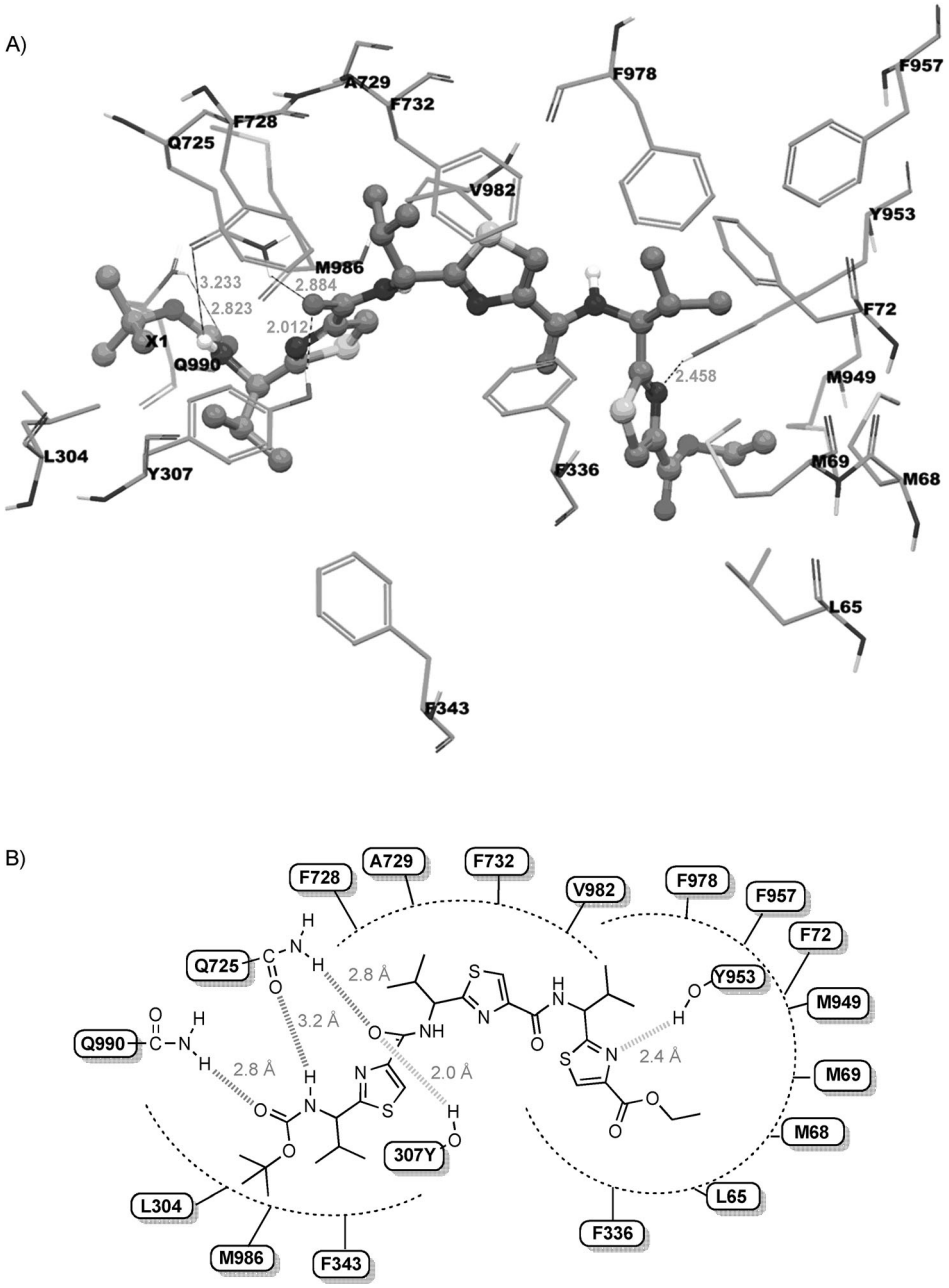

Figure 3. XP-Glide-predicted binding mode of compound **13** with homology modeled P-gp. A) 3D model of the binding mode of linear trimer **13** in the homology modeled human P-gp drug binding cavity. Important amino acids present within 4 Å from the ligand are depicted as sticks with the atoms colored as: carbon: green, hydrogen: white, nitrogen: blue, oxygen: red, sulfur: yellow), whereas the inhibitor is shown as a ball-and-stick model with the same color scheme as above except that carbon atoms are represented in orange. Electrostatic and hydrogen bonding interactions are shown in Å with the distances in dotted lines. B) Schematic representation diagram of the 3D model with important interactions observed in the complex of liner trimer **13** with the drug binding site residues of human P-gp. Electrostatic (blue dotted lines) and hydrogen bonding (red dotted lines) interactions are shown with distances in Å. (For the references to color in this figure legend, the reader is referred to the Supporting Information.)

Experimental Section

Chemistry–general: Chemicals were purchased from Aldrich, AK Scientific (Union City, CA), Oakwood Products (West Columbia, SC), Alfa Aesar (Ward Hill, MA), and TCI America (Portland, OR) and were used as received. All compounds were checked for homogeneity by TLC with silica gel as the stationary phase. Melting points were determined on a Thomas Hoover capillary melting point apparatus and are uncorrected. NMR spectra were recorded on a Bruker 400 Avance DPX spectrometer (^{1}H at 400 MHz) outfitted with a *z*-axis gradient probe. The chemical shifts (δ) for ^{1}H NMR are reported in parts per million (ppm) downfield from tetramethylsilane (TMS) as an internal standard. Flash chromatography was performed by using silica gel (0.060–0.200 mm) obtained from Dynamic adsorbents. HPLC was performed by using an Agilent 1260 Infinity system employing a Dynamax silica gel cartridge column (30 cm × 10 mm internal diameter). Elutions were monitored at UV = 254 nm. Optical rotations of the chiral compounds were measured on a PerkinElmer 241 Polarimeter with chloroform as solvent; concentration (*c*) is expressed as g/100 mL. Chiral HPLC analysis was performed on a Dionex Ultimate 3000 Series instrument. The compounds were dissolved in MeOH and injected (20 μL each) into a Chiralpak 1A column (Daicel Corp., Fort Lee, NJ) with stationary phase as amylose tris (3,5-dimethylphenylcarbamate) immobilized on 5 μm silica gel. Chiral homogeneity was ensured by using an isocratic mobile phase (*n*-hexane/EtOAc 1:1), eluting at a flow rate of 1 mL min^{-1} and monitored at UV = 370 nm.

Synthesis

Method A: General procedures for ester hydrolysis of thiazole amino acid derivatives: Thiazole ethyl ester derivatives (0.01 M) were added in a mixture of solvents [THF/MeOH/water (10:2:3)], and cooled to 0 °C. NaOH (10 equiv) was added, and the mixture was stirred at RT for 12 h. The reaction mixture was then concentrated in vacuo and partitioned between EtOAc (30 mL) and water (20 mL). The aqueous phase containing compound was collected and acidified to pH 4 with 10% $KHSO_4$, then extracted with EtOAc (3 × 20 mL). The organic fractions were dried over sodium sulfate (Na_2SO_4) and concentrated under reduced pressure to yield the carboxylic acid derivatives.

Method B: General procedures for Boc-N-deprotection of thiazole amino acid derivatives: Trifluoroacetic acid (TFA; 42 equiv) was added dropwise to a solution of *N*-Boc protected thiazoles in

CH_2Cl_2 (1 mL mmol^{-1}) at 0 °C and the solution was stirred at RT under nitrogen atmosphere for 12 h. After completion of the reaction, the solvent was removed in vacuo, followed by coevaporation of the residual solvent with toluene (3×30 mL). The remaining crude mass was added to water (20 mL), acidified with 2 M HCl, and extracted with EtOAc (30 mL). Saturated aqueous $NaHCO_3$ was added to the aqueous phase containing amine salt and extracted with EtOAc (3×30 mL). The organic layers were washed with brine, dried over Na_2SO_4, and evaporated. The resulting concentrate was triturated with diethyl ether and dried in vacuo to afford free amine derivatives.

Method C: General procedures for peptide coupling to obtain linear thiazole derivatives: Di-isopropylethylamine (DIEA; 1.5 equiv) was added to the stirred suspension of the carboxylic acid derivatives (1.0 equiv) in 4:1 CH_2Cl_2/DMF (0.25 M) or dimethyl acetamide (DMA; 0.10 M). The mixture was cooled to 0 °C, then BOP reagent (1.5 equiv) in DMF or HCTU (1.5 equiv) in DMA, followed by HOBt (1.5 equiv), were added. The solution was stirred at 0 °C for 10 min, then a pre-cooled solution of the thiazole amine TFA salt (1.3–1.5 equiv) in DMF (or DMA) and DIEA (1.5 equiv) was added and stirred at RT for 12–15 h. The reaction mixture was then concentrated in a vacuum rotary evaporator, followed by partitioning of the residual mass between EtOAc and aqueous citric acid (10%, *w/v*). The aqueous layer was repeatedly extracted with EtOAc (4× 20 mL). The combined organic fractions were washed sequentially with saturated aqueous $NaHCO_3$ and brine. This mixture was then dried over Na_2SO_4 with subsequent evaporation under reduced pressure. The residue was purified by flash chromatography on silica gel with *n*-hexane/EtOAc (1:1) as eluent to give the required compounds.

Method D: General procedures for cyclization through peptide coupling of thiazole amino acids: The zwitterion derivatives were suspended in a mixture of anhydrous CH_2Cl_2/DMF (4:1; 20 mL mmol^{-1}) under inert atmosphere with subsequent addition of DIEA (3 equiv), pentafluorophenyl diphenylphosphinate (FDPP; 3 equiv) and anhydrous $ZnCl_2$ (1 equiv; to induce cyclization of the trimer).[28] The reaction mixture was stirred at RT and monitored by TLC. Upon disappearance of the starting compound (five days), the reaction was quenched with saturated aqueous $NaHCO_3$, and the solvent was concentrated in vacuo. The residual mixture was partitioned between CH_2Cl_2 (50 mL) and water (25 mL). The aqueous fraction was back-extracted with CH_2Cl_2 (2×50 mL), and combined organic layers were washed successively with 10% aqueous citric acid (2×25 mL), water (25 mL) and brine (50 mL), dried over Na_2SO_4, and evaporated under reduced pressure to leave a mixture of cyclic peptide products, which were separated by silica gel column chromatography (EtOAc/*n*-hexane 7:3) or by preparative HPLC with a gradient solvent system (60–90% CH_3CN in mixture of 0.1% TFA in water) with a flow rate of 1 mL min^{-1} to obtain the pure cyclic peptides.

(*S*)-(1-Carbamoyl-2-methylpropyl)carbamic acid *tert*-butyl ester (2): Isobutyl chloroformate (2.26 g, 16.56 mmol) and *N*-methylmorpholine (NMM; 1.68 g, 16.56 mmol) were added to a stirred solution of *N*-Boc-(*S*)-valine (**1**; 3.00 g, 13.80 mmol) in anhydrous THF (20 mL) under nitrogen atmosphere and was allowed to stir for 4 h at −20 °C. Afterwards, excess (20 mL) of aqueous ammonia (30%) was added, and the resulting biphasic mixture was stirred at room temperature for 4 h. After completion of the reaction, THF was removed under reduced pressure. The residual mixture was extracted with EtOAc (3×30 mL). The combined organic fractions were washed with 1 N $KHSO_4$ and brine, then dried over anhydrous Na_2SO_4. After evaporation of the solvent, the product was recrystallized by trituration with EtOAc/*n*-hexane (3:8) to provide the amide (**2**) as a white solid (2.87 g, 96%): m.p. 156–159 °C (lit. 160–161 °C);[25] ^{1}H NMR (400 MHz; [D$_6$]DMSO; TMS): δ = 7.29 (s, 1 H), 7.03 (s, 1 H), 6.54 (d, J = 8.9 Hz, 1 H), 3.73 (t, J = 8.9 Hz, 1 H), 1.91–1.89 (m, 1 H), 1.38 (s, 9 H), 0.85 (d, J = 7.1 Hz, 3 H), 0.81 ppm (d, J = 7.1 Hz, 3 H).

(*S*)-(2-Methyl-1-thiocarbamoylpropyl)carbamic acid *tert*-butyl ester (3): Compound **2** (2.50 g, 11.56 mmol) was dissolved in dry THF (30 mL) under nitrogen atmosphere. Lawesson's reagent (9.35 g, 23.12 mmol) was added under a well-ventilated fume hood, and the resulting suspension was stirred at 50 °C for 16 h. After cooling to RT, the reaction was quenched with saturated aqueous $NaHCO_3$ (20 mL), then diluted with EtOAc (40 mL) and stirred at RT for additional 2 h. The layers were separated, and the organic layer was washed with brine (20 mL), dried over Na_2SO_4, and concentrated in vacuo. Purification by flash column chromatography (5–25% EtOAc/*n*-hexane) yielded title compound (**3**) as a yellow solid (2.15 g, 80%): m.p. 72–76 °C (lit. 84–85 °C);[21] R_f = 0.6 (EtOAc/*n*-hexane 2:3); ^{1}H NMR (400 MHz; [D$_6$]DMSO; TMS): δ = 9.63 (s, 1 H), 9.18 (s, 1 H), 6.52 (d, J = 9.1 Hz, 1 H), 3.55–3.53 (m, 1 H), 1.90–1.88 (m, 1 H), 1.43 (s, 9 H), 0.87 (d, J = 7.1 Hz, 3 H), 0.84 ppm (d, J = 7.1 Hz, 3 H).

(*S*)-2-(1-*tert*-Butoxycarbonylamino-2-methylpropyl)thiazole-4-carboxylic acid ethyl ester (5):[23] The solution of **3** (2.00 g, 8.61 mmol) in dry DME (30 mL) was cooled to −15 °C with subsequent addition of $KHCO_3$ (7.76 g, 77.49 mmol) under nitrogen atmosphere. The resulting suspension was vigorously stirred for 15 min, followed by dropwise addition of ethyl bromopyruvate (2.01 g, 10.33 mmol) under inert atmosphere. The reaction was then continued at −15 °C for 1 h after which it was allowed to warm gradually to RT and stirred for 12 h. The mixture was then filtered through a celite pad. The filtrate was concentrated in vacuo at 40 °C to yield a dark colored crude mass of hydroxythiazoline intermediate **4**. The crude mass was further dissolved per se in dry DME (20 mL) under nitrogen, and the resulting solution was cooled to −15 °C. To this, a solution of 2,6-lutidine (7.38 g, 68.88 mmol) and TFAA (9.04 g, 43.05 mmol) in dry DME (10 mL) was added dropwise over a period of 40 min (large amounts of CO_2 were released). The solution was stirred at −15 °C for 3 h and then allowed to stir at RT for an additional 12 h; afterwards, the reaction mixture was concentrated and then stirred with freshly prepared sodium ethoxide (3 equiv) in EtOH (20 mL). After 6 h, EtOH was evaporated under reduced pressure. The residual product was added to a saturated aqueous $NaHCO_3$ (10 mL) solution. The resulting mixture was extracted with EtOAc (3×30 mL). The combined organic layer was washed with citric acid (10%) and brine, dried over Na_2SO_4, and concentrated in vacuo. Purification of the residue by column chromatography (5–35% EtOAc/*n*-hexane) afforded the title compound (**5**) as a white solid (1.04 g, 37%): m.p. 112–114 °C (lit. 114–116 °C);[21] R_f = 0.5 (EtOAc/*n*-hexane 2:3); purity (HPLC, UV = 254 nm): 95%; ^{1}H NMR (400 MHz; [D$_6$]DMSO; TMS): δ = 8.40 (s, 1 H), 7.72 (d, J = 8.4 Hz, 1 H), 4.61 (t, J = 7.5 Hz, 1 H), 4.31–4.27 (m, 2 H), 2.21–2.19 (m, 1 H) 1.39 (s, 9 H), 1.29 (t, J = 7.1 Hz, 3 H), 0.88 (d, J = 6.7 Hz, 3 H), 0.84 ppm (d, J = 6.7 Hz, 3 H).

(*S*)-2-(1-*tert*-Butoxycarbonylamino-2-methylpropyl)thiazole-4-carboxylic acid (6): Compound **5** (0.90 g, 2.74 mmol) was hydrolyzed to obtain compound **6**, according to method A, as a white solid (0.75 g, 91%): m.p. 131–133 °C; R_f = 0.20 (MeOH/CH_2Cl_2 5:95); purity (HPLC, UV = 254 nm): 97%; ^{1}H NMR (400 MHz; [D$_6$]DMSO; TMS): δ = 12.34 (s, 1 H), 8.32 (s, 1 H), 7.70 (d, J = 8.4 Hz, 1 H), 4.60 (t, J = 7.5 Hz, 1 H), 2.21–2.19 (m, 1 H) 1.39 (s, 9 H), 0.88 (d, J = 6.7 Hz, 3 H), 0.84 ppm (d, J = 6.7 Hz, 3 H).

(*S*)-2-(1-Amino-2-methylpropyl)thiazole-4-carboxylic acid ethyl ester (7): Compound **5** (0.80 g, 3.50 mmol) was used to obtain compound **7** as a yellow solid (0.47 g, 85%) by using Method B: m.p. 38–39 °C; R_f = 0.30 (MeOH/CH_2Cl_2 5:95); purity (HPLC, UV 254 nm): 95%; ^{1}H NMR (400 MHz; [D$_6$]DMSO; TMS): δ = 8.50 (s, 1H), 5.10–4.80 (m, 1H), 4.39 (q, J = 7.0 Hz, 2H), 2.44–2.42 (m, 1H), 2.1 (br s, 2H), 1.38 (t, J = 7.0 Hz, 3H), 0.89 (d, J = 6.7 Hz, 3H), 0.86 ppm (d, J = 6.8 Hz, 3H).

(*S*)-2-(1-Amino-2-methylpropyl)thiazole-4-carboxylic acid (8): Compound **6** (0.50 g, 1.66 mmol) was first dissolved in CH_2Cl_2 (15 mL) under nitrogen atmosphere and cooled to 0 °C. TFA (42 equiv) was added dropwise, and the solution was stirred at RT under nitrogen atmosphere for 12 h. After removal of CH_2Cl_2, the residual mixture was coevaporated with toluene (3×10 mL) to obtain the salt form of compound **8**, which was used without further purification.

(*S*)-2-(1-{[2-(1-*tert*-Butoxycarbonylamino-2-methylpropyl)thiazole-4-carbonyl]amino}-(*S*)-2-methylpropyl)thiazole-4-carboxylic acid ethyl ester (9): Dimer **9** was obtained from compounds **6** (0.45 g, 1.99 mmol) and **7** (0.50 g, 1.66 mmol), by following Method C, as a white solid (0.45 g, 53%): m.p. 90–92 °C (lit. 91–93 °C);[20] R_f = 0.40 (EtOAc/*n*-hexane 2:3); purity (HPLC, UV = 254 nm): 98%; ^{1}H NMR (400 MHz; [D$_6$]DMSO; TMS): δ = 8.73 (d, J = 8.4 Hz, 1H), 8.46 (s, 1H), 8.23 (s, 1H), 7.74 (t, J = 6.9 Hz, 1H), 5.15–5.06 (m, 1H), 4.70 (br s, 1H), 4.32 (q, J = 7.0 Hz, 2H), 2.47–2.45 (m, 1H), 2.24–2.22 (m, 1H), 1.40 (s, 9H), 1.30 (t, J = 7.1 Hz, 3H), 0.97 (d, J = 6.8 Hz, 3H), 0.90–0.88 ppm (m, 9H); ESI-MS(+): *m/z* found for $C_{23}H_{34}N_4O_5S_2Na$: 533.18 [M+Na]$^+$.

(*S*)-2-(1-{[2-(1-*tert*-Butoxycarbonylamino-2-methylpropyl)thiazole-4-carbonyl]amino}-(*S*)-2-methylpropyl)thiazole-4-carboxylic acid (10): Dimer acid **10** was obtained, by hydrolyzing dimer **9** (0.40 g, 0.78 mmol) according to Method A, as a white solid (0.33 g, 79%): m.p. 101–103 °C (lit. 101–106 °C);[20] R_f = 0.20 (MeOH/CH_2Cl_2 5:95); purity (HPLC, UV = 254 nm) > 99%; ^{1}H NMR (400 MHz; [D$_6$]DMSO; TMS): δ = 8.69 (d, J = 8.4 Hz, 1H), 8.38 (s, 1H), 8.23 (s, 1H), 7.74 (d, J = 8.1 Hz, 1H), 5.11 (t, J = 8.4 Hz, 1H), 4.70 (t, J = 7.6 Hz, 1H), 2.47–2.45 (m, 1H), 2.25–2.23 (m, 1H), 1.40 (s, 9H), 0.97 (d, J = 6.8 Hz, 3H), 0.92–0.85 ppm (m, 9H) (acid peak was missing); ESI-MS(+): *m/z* found for $C_{21}H_{30}N_4O_5S_2Na$: 505.15 [M+Na]$^+$.

(*S*)-2-(1-{[2-(1-Amino-2-methylpropyl)thiazole-4-carbonyl]amino}-(*S*)-2-methylpropyl)thiazole-4-carboxylic acid ethyl ester (11): Dimer amine **11** was obtained from dimer **9** (0.40 g, 0.78 mmol), by following Method B, as a yellowish-white solid (0.12 g, 36%): m.p. 119–122 °C (lit. 120–123 °C);[20] R_f = 0.20 (MeOH/CH_2Cl_2 5:95); purity (HPLC, UV = 254 nm): 95%; ^{1}H NMR (400 MHz; CD_3OD; TMS): δ = 8.62 (d, J = 8.7 Hz, 1H), 8.42 (s, 1H), 8.21 (s, 1H), 5.15–5.11 (m, 2H), 4.32 (q, J = 7.1 Hz, 2H), 2.47–2.40 (m, 2H), 1.30 (t, J = 7.1 Hz, 3H), 1.16 ppm (m, 12H) (amine peak was missing); ESI-MS(+): *m/z* found for $C_{18}H_{26}N_4O_3S_2Na$: 433.18 [M+Na]$^+$.

(*S*)-2-(1-{[2-(1-Amino-2-methylpropyl)thiazole-4-carbonyl]amino}-(*S*)-2-methylpropyl)thiazole-4-carboxylic acid (12): TFA (42 equiv) was added dropwise to the suspension of dimer acid **10** (0.30 g, 0.62 mmol) in CH_2Cl_2 (15 mL) at 0 °C. After completion of the reaction, the solvent was coevaporated with toluene (45 mL). The crude mass was dissolved in EtOAc and washed with 10% aqueous $NaHCO_3$ (2×10 mL) and brine (2×10 mL). The organic extract was dried over Na_2SO_4 and concentrated in vacuo. The residual mass was triturated with ether and hexane to afford the title compound **12** as a white solid (0.21 g, 86%): R_f = 0.20 (MeOH/CH_2Cl_2 5:95); purity (HPLC, UV = 254 nm): 98%; ^{1}H NMR (400 MHz; [D$_6$]DMSO; TMS): δ = 8.69 (t, J = 8.9 Hz, 1H), 8.45 (d, J = 3.3 Hz, 1H), 8.40 (s, 1H), 5.18–5.12 (m, 1H), 4.70 (t, J = 7.6 Hz, 1H), 2.47–2.45 (m, 1H), 2.25–2.3 (m, 1H), 1.01–0.90 ppm (m, 12H) (amine and acid peaks were missing); ESI-MS(+): *m/z* found for $C_{16}H_{22}N_4O_3S_2Na$: 382.11 [M+Na]$^+$.

(*S*)-2-(1-{[2-(1-{[2-(1-*tert*-Butoxycarbonylamino-2-methylpropyl)thiazole-4-carbonyl]amino}-(*S*)-2-methylpropyl)thiazole-4-carbonyl]amino}-(*S*)-2-methylpropyl)thiazole-4-carboxylic acid ethyl ester (13): Linear trimer **13** was obtained from dimer acid **10** (0.30 g, 0.62 mmol) and monomer amine **7** (0.17 g, 0.74 mmol), by following Method C, as a white solid (0.16 g, 36%): R_f = 0.40 (EtOAc/*n*-hexane 1:1); purity (HPLC, UV 254 nm): 98%; ^{1}H NMR (400 MHz; $CDCl_3$; TMS): δ = 8.07 (s, 1H), 8.06 (s, 1H), 8.04 (s, 1H), 7.95 (d, J = 9.2 Hz, 1H), 7.82 (d, J = 9.2 Hz, 1H), 5.39–5.32 (m, 2H), 5.11 (d, J = 8.7 Hz, 1H), 4.89 (br s, 1H), 4.43 (q, J = 7.1 Hz, 2H), 2.71–2.60 (m, 2H), 2.41–2.30 (m, 1H), 1.45 (s, 9H), 1.40 (t, J = 7.1 Hz, 3H), 1.08–1.00 (m, 15H), 0.94–0.87 ppm (d, J = 6.8 Hz, 3H); ESI-MS(+): *m/z* found for $C_{31}H_{45}N_6O_6S_3$: 693.26 [M+H]$^+$.

(*S*)-2-(1-{[2-(1-{[2-(1-*tert*-Butoxycarbonylamino-2-methylpropyl)thiazole-4-carbonyl]amino}-(*S*)-2-methylpropyl)thiazole-4-carbonyl]amino}-(*S*)-2-methylpropyl)thiazole-4-carboxylic acid (14): Trimer acid **14** was obtained from linear trimer **13** (0.30 g, 0.43 mmol), by following Method A, as a white solid (0.24 g, 83%): R_f = 0.20 (MeOH/CH_2Cl_2 5:95); purity (HPLC, UV 254 nm): 98%; ^{1}H NMR (400 MHz; [D$_6$]DMSO; TMS): δ = 12.95 (s, 1H), 8.73 (s, 2H), 8.38 (s, 1H), 8.28 (d, J = 5.6 Hz, 1H), 8.23 (br s, 1H), 7.74 (d, J = 9.2 Hz, 1H), 5.18 (d, J = 8.7 Hz, 2H), 4.68 (br s, 1H), 2.47–2.31 (m, 2H), 2.24–2.21 (m, 1H), 1.41 (s, 9H), 1.04–0.86 ppm (m, 18H); ESI-MS(+): *m/z* found for $C_{29}H_{40}N_6O_6S_3Na$: 687.21 [M+Na]$^+$.

(*S*)-2-(1-{[2-(1-{[2-(1-Amino-2-methylpropyl)thiazole-4-carbonyl]amino}-(*S*)-2-methylpropyl)thiazole-4-carbonyl]amino}-(*S*)-2-methylpropyl)thiazole-4-carboxylic acid ethyl ester (15): Trimer amine **15** was obtained from linear trimer **13** (0.40 g, 0.58 mmol), by following Method B, as a white solid (0.11 g, 31%): R_f = 0.20 (MeOH/CH_2Cl_2 5:95); purity (HPLC, UV 254 nm): 95%; ^{1}H NMR (400 MHz; [D$_6$]DMSO; TMS): δ = 8.74–8.68 (m, 2H), 8.62 (br s, 2H), 8.47 (s, 2H), 8.30 (s, 1H), 5.21–5.10 (m, 2H), 4.74 (br s, 1H), 4.29 (q, J = 7.1 Hz, 2H), 2.47–2.31 (m, 2H), 2.29–2.27 (m, 1H), 1.28 (t, J = 7.1 Hz, 3H), 1.32–0.87 ppm (m, 18H); ESI-MS(+): *m/z* 593.00 ($C_{26}H_{37}N_6O_4S_3$, 593.20, [M+H]$^+$).

(*S*)-2-(1-{[2-(1-{[2-(1-Amino-2-methylpropyl)thiazole-4-carbonyl]amino}-(*S*)-2-methylpropyl)thiazole-4-carbonyl]amino}-(*S*)-2-methylpropyl)thiazole-4-carboxylic acid (16): TFA (42 equiv) was added dropwise to a solution of trimer acid **14** in CH_2Cl_2 (15 mL) at 0 °C, and the solution was stirred at RT under nitrogen atmosphere for 15 h. After completion of the reaction, the solvent was coevaporated with toluene (3×). The resulting product was used without further purification. ESI-MS(+): *m/z* found for $C_{24}H_{33}N_6O_4S_3$: 565.18 [M+H]$^+$.

Cyclic tris-thiazole amino acid (QZ59S-SSS; 17): Compound **17** was obtained from compound **16** (0.80 g, 1.42 mmol), by following Method D, as a white solid (0.25 g, 32%): m.p. 243–247 °C; R_f = 0.45 (EtOAc/*n*-hexane 1:1); purity (HPLC, UV = 254 nm) ≥ 98%; $[\alpha]_D^{25}$ = −102.64° (c = 5.3, $CHCl_3$); ^{1}H NMR (400 MHz; $CDCl_3$; TMS): δ = 8.47 (d, J = 9.1 Hz, 3H), 8.09 (s, 3H), 5.43 (dd, J = 9.3 Hz, 5.8 Hz, 3H), 2.34–2.27 (m, 3H), 1.10 (d, J = 6.8 Hz, 9H), 1.05 ppm (d, J = 6.8 Hz, 9H); ESI-MS(+): *m/z* found for $C_{24}H_{31}N_6O_3S_3$: 547.15 [M+H]$^+$.

Preparation of 17 through coupling and cyclization of 8: Alternatively, compound **17** was obtained from compound **8** (0.75 g, 2.45 mmol) as a white solid (0.11 g, 24%), by following method D.

(*S*)-2-(1-{[2-(1-{[2-(1-{[2-(1-*tert*-Butoxycarbonylamino-2-methylpropyl)thiazole-4-carbonyl]amino}-(*S*)-2-methylpropyl)thiazole-4-

carbonyl]amino}-(*S*)-2-methylpropyl)thiazole-4-carbonyl]amino}-(*S*)-2-methylpropyl)thiazole-4-carboxylic acid ethyl ester (18): Dimer acid **10** (0.40 g, 0.46 mmol) and dimer amine **11** (0.23 g, 0.55 mmol) were coupled according to Method C to give linear tetramer **18** as a white solid (0.23 g, 32%): purity (HPLC, UV = 254 nm): 98%; ^{1}H NMR (400 MHz; [D$_6$]DMSO; TMS): δ = 8.77–8.70 (m, 3H), 8.45 (s, 1H), 8.27 (brs, 2H), 8.23 (s, 1H), 7.76 (d, J = 7.9 Hz, 1H), 5.19–5.07 (m, 3H), 4.70 (brs, 1H), 4.28 (q, J = 7.2 Hz, 2H), 2.47–2.42 (m, 3H), 2.27–2.23 (m, 1H), 1.39 (s, 9H), 1.31 (t, J = 7.1 Hz, 3H), 1.10–0.95 (m, 9H), 0.94–0.82 ppm (m, 15H); ESI-MS(+): *m/z* found for $C_{39}H_{54}N_8O_7S_4Na$: 897.2871 [M+Na]$^+$.

Linear hexamer (19): The trimer acid (**14**; 0.10 g, 0.15 mmol) and the trimer amine (**15**; 0.11 g, 0.18 mmol) were coupled according to Method C, and the crude product was purified by preparative HPLC with a gradient solvent system of 60–90% CH_3CN in water with 0.1% TFA. The peak separated at 51 min was characterized as linear hexamer **19** by ESI-MS analysis and obtained as a white solid (0.002 g, 0.60%): purity (HPLC, UV = 254 nm) $\geq$99%; ESI-MS(+): *m/z* found for $C_{55}H_{74}N_{12}O_9S_6Na$: 1261.48 [$M$+Na]$^+$.

Cyclic tetramer 20 and cyclic hexamer 21: Cyclic tetramer **20** and cyclic hexamer **21** were obtained from dimer zwitterions (0.90 g, 2.74 mmol) by following Method D and were separated by preparative HPLC with a gradient solvent system of 60–90% CH_3CN in water with 0.1% TFA at a flow rate of 1 mL min^{-1}. Both compounds were confirmed by single peaks in the ESI-MS spectrum. The extremely low yield of cyclic hexamer permitted us to evaluate ESI-MS and biological activity only.

Cyclic tetramer 20: The peak separated at 19 min was cyclic tetramer **20** (0.001 g, 0.11%): m.p. 150–153 °C; R_f = 0.45 (EtOAc/*n*-hexane 2:1); purity (HPLC, UV = 254 nm): 99%; ^{1}H NMR (400 MHz; $CDCl_3$; TMS): δ = 8.66 (d, J = 8.9 Hz, 1H), 8.31 (d, J = 8.6 Hz, 1H), 8.18 (s, 1H), 8.15 (brs, 2H), 8.13 (s, 1H), 8.01 (d, J = 7.3 Hz, 1H), 7.89 (d, J = 10.0 Hz, 1H), 5.52–5.48 (m, 1H), 5.36 (t, J = 9.8 Hz, 1H), 5.25 (t, J = 7.8 Hz, 1H), 5.03 (t, J = 7.8 Hz, 1H), 2.69–2.67 (m, 1H), 2.43–2.41 (m, 2H), 2.29–2.27 (m, 1H), 1.23 (d, J = 6.7 Hz, 3H) 1.17 (d, J = 6.7 Hz, 3H), 1.12 (d, J = 6.52 Hz, 3H), 1.07 (d, J = 6.8 Hz, 3H), 1.04–0.90 (m, 9H), 0.87 ppm (d, J = 6.7 Hz, 3H); ESI-MS(+): *m/z* found for $C_{32}H_{41}N_8O_4S_4$: 729.00 [M+H]$^+$.

Cyclic hexamer 21: The peak separated at 55 min was cyclic hexamer **21** (0.001 g, 0.11%): purity (HPLC, UV = 254 nm) $\geq$98%; ESI-MS(+): *m/z* found for $C_{48}H_{60}N_{12}O_6S_6$: 1094 [M+H]$^+$.

{1-[4-(1-{4-[(*R*)-(+)-1-(4-Methoxyphenyl)ethylcarbamoyl]thiazol-2-yl}-(*S*)-2-methylpropylcarbamoyl)thiazol-2-yl]-(*S*)-2-methylpropyl}carbamic acid *tert*-butyl ester (22): Compounds **10** (0.10 g, 0.21 mmol) and **22a** (0.06 g, 0.42 mmol) were reacted together by following Method C with HCTU to obtain compound **22** as a yellowish-white solid (0.08 g, 63%): m.p. 64–66 °C; R_f = 0.55 (EtOAc/*n*-hexane 1:1); purity (HPLC, UV = 254 nm): 96%; ^{1}H NMR (400 MHz; $CDCl_3$; TMS): δ = 8.66–8.61 (m, 1H), 8.43–8.36 (m, 1H), 8.22 (s, 1H), 8.16 (s, 1H), 7.74 (d, J = 7.8 Hz, 1H), 7.32 (d, J = 8.4 Hz, 2H), 6.88 (d, J = 8.4 Hz, 2H), 5.18–5.08 (m, 2H), 4.70–4.66 (m, 1H), 3.72 (s, 3H), 2.47–2.44 (m, 1H), 2.27–2.21 (m, 1H), 1.48 (d, J = 6.9 Hz, 3H), 1.40 (s, 9H), 0.97 (d, J = 6.2 Hz, 3H), 0.90–0.86 ppm (m, 9H); ESI-MS(+): *m/z* found for $C_{30}H_{41}N_5O_5S_2Na$: 638.2430 [M+Na]$^+$.

[1-(4-{1-[4-(2,4-Dimethoxybenzylcarbamoyl)thiazol-2-yl]-(*S*)-2-methylpropylcarbamoyl}thiazol-2-yl)-(*S*)-2-methylpropyl]carbamic acid *tert*-butyl ester (23): Compounds **10** (0.10 g, 0.21 mmol) and **23a** (0.07 g, 0.42 mmol) were reacted together according to Method C by using HCTU to obtain compound **23** as a white solid (0.09 g, 68%): m.p. 70–74 °C; R_f = 0.55 (EtOAc/*n*-hexane 1:1); purity (HPLC, UV 254 nm): 98%; ^{1}H NMR (400 MHz; [D$_6$]DMSO; TMS): δ = 8.68 (brs, 1H), 8.39 (d, J = 5.8 Hz, 1H), 8.23 (s, 1H), 8.19 (d, J = 3.6 Hz, 1H), 7.75 (brs, 1H), 7.08 (d, J = 8.2 Hz, 1H), 6.56 (s, 1H), 6.47 (d, J = 8.4 Hz, 1H), 5.17–5.07 (m, 1H), 4.69–4.67 (m, 1H), 4.37 (d, J = 5.8 Hz, 2H), 3.80 (s, 3H), 3.73 (s, 3H), 2.48–2.46 (m, 1H), 2.25–2.22 (m, 1H), 1.40 (s, 9H), 1.12–1.05 ppm (m, 12H); ESI-MS(+): *m/z* found for $C_{30}H_{41}N_5O_6S_2Na$: 654.2399 [M+Na]$^+$.

Biological procedures

Cell lines: HeLa cells were cultured in Dulbecco's modified Eagle's medium (DMEM) supplemented with 10% fetal bovine serum (FBS), 1% glutamine, and 1% penicillin as described previously.[3]

Cloning and amplification of BacMam-P-gp virus and transduction of HeLa cells: The expression clones for P-gp were generated in pDest-625, as described previously.[3] These were then transformed into *E. coli* DH10Bac cells (Invitrogen) and plated on gentamycin-, kanamycin-, tetracycline-, IPTG-, and X-gal-selective media as per the manufacturers' protocols. White colonies were then selected from these plates, and bacmid DNA was prepared by the alkaline lysis method, which was further verified by PCR amplification across the bacmid junctions.

HeLa cells (2.5 million) were transduced with BacMam WT-P-gp virus at a titer of 50–60 viral particles per cell in DMEM (3 mL).[3] DMEM (17 mL) was added after 1 h, and the cells were further incubated at 37 °C in 5% CO_2. After 3–4 h, 10 mM butyric acid was added, and the cells were grown overnight at 37 °C. After 24 h, the cells were trypsinized, washed, counted, and analyzed by flow cytometry to test the potency of various derivatives to inhibit transport function of P-gp.

Fluorescent substrate transport assay: The ability of various derivatives to inhibit the transport function of human P-gp was evaluated with fluorescent substrates by flow cytometry, as described previously.[41,42] Briefly, the baculovirus-transduced cells were trypsinized and resuspended in IMDM medium containing 5% FBS. Cells were incubated with the indicated concentration of the compounds or 1 μM tariquidar, followed by calcein-AM (0.5 μM) for 10 min or BODIPY-FL-Prazosin (0.5 μM) for 45 min at 37 °C, as described previously.[3] The cells were washed with cold PBS, resuspended in 300 μL of PBS with 0.1% bovine serum albumin, and analyzed. Fluorescence of calcein or BODIPY-FL-Prazosin was measured with a FACSort flow cytometer, equipped with a 488 nm argon laser and 530 nm bandpass filter. The percentage of transport inhibition was derived when compared with inhibition obtained by using the standard inhibitor, tariquidar, at 1 μM. The results are plotted as an average of two experiments. The IC_{50} values for inhibition of calcein-AM efflux by selected derivatives were calculated by using GraphPad Prism 5.0.

Photoaffinity labeling of P-gp with [^{125}I]IAAP: Crude membranes (1 mg protein per mL) from P-gp-expressing High-Five insect cells were photolabeled with [^{125}I]IAAP (2200 Ci mmol^{-1}) in the absence or presence of tested compounds, as described previously.[43] Briefly, crude membranes from P-gp-expressing High-Five insect cells were incubated in the presence and absence of 10 μM thiazole derivatives or 5 μM tariquidar in 50 mM Tris·HCl (pH 7.5) and 6 nM [^{125}I]IAAP (2200 Ci mmol^{-1}). The samples were then photo-crosslinked, and images were developed on a phosphorimager. The radioactivity associated with the P-gp band was quantified, and percent inhibition of IAAP incorporation was calculated. The results are given as percent inhibition as an average of two independent experiments.

ATPase assay: Crude membrane protein (100 μg protein mL^{-1}) from High-Five insect cells expressing P-gp was incubated at 37 °C with

thiazole derivatives (2.5 μM) or verapamil (50 μM) in the presence and absence of 0.3 mM sodium orthovanadate, and ATP hydrolysis was measured as described previously.[44] The vanadate-sensitive ATPase activity is expressed as nanomoles $P_i\,min^{-1}\,mg^{-1}$ protein.

Molecular modeling

Ligand preparation: The structures of (*S*)-valine-based thiazole derivatives were built by using the fragment dictionary of Maestro v9.0, and subsequent energy minimization was performed by the Macromodel program v9.7 (Schrödinger, Inc., New York, NY, 2009). Low-energy 3D structures of compounds were generated by LigPrep v2.3 as described previously.[13]

Protein preparation: The X-ray crystal structure of mouse P-gp in the apo state (PDB ID: 3G5U) and in complex with inhibitors QZ59Se-*RRR* (PDB ID: 3G60), QZ59Se-*SSS* (PDB ID: 3G61)[5] and ATP-bound (PDB ID: 1MV5), obtained from the RCSB Protein Data Bank, were used to build the homology model of human ABCB1. The protocol for homology modeling is essentially the same as reported previously.[13] The refined human P-gp homology model was further used to generate different receptor grids by selecting QZ59Se-*RRR* (site 1) and QZ59Se-*SSS* (site 2) bound ligands, all amino acid residues known to contribute to verapamil binding (site 3), two residues (F728 and V982) known to be common to sites 1–3 (site 4) and the ATP binding site. Derivatives were docked on all of the mentioned sites for comparison.

Docking protocol: A conformational library of ligands was docked at each of the generated grids (sites 1 to 4 and the ATP binding site of P-gp by using the "Extra Precision" (XP) mode of Glide program v5.0 (Schrödinger, Inc., New York, NY, 2009) with the default functions. The top scoring ligand's conformation was used for graphical analysis. All computations were carried out on a Dell Precision 470n dual processor with Linux OS (Red Hat Enterprise WS 4.0).

Acknowledgements

This research was supported by the Department of Pharmaceutical Sciences of St. John's University and St. John's University Seed Grant No. 579-1110 (to T.T.T.). N.R.P., K.K., E.E.C., and S.V.A. were supported by the Intramural Research Program of the NIH, National Cancer Institute, Center for Cancer Research. Financial support from the Indian Council of Medical Research, New Delhi in the form of an International Fellowship for Young Indian Biomedical Scientists to N.R.P. is gratefully acknowledged (Indo/FRC/452(Y-19)/2012-13IHD). S.S. and T.T.T. are thankful to Dr. Sanjai Kumar and Dibyendu Dana for assisting in preparative HPLC, ESI-MS, and chiral HPLC analyses.

Keywords: ABC transporters · molecular modeling · multidrug resistance · peptide mimics · P-glycoprotein

[1] S. V. Ambudkar, S. Dey, C. A. Hrycyna, M. Ramachandra, I. Pastan, M. M. Gottesman, *Annu. Rev. Pharmacol. Toxicol.* **1999**, *39*, 361–398.
[2] A. H. Schinkel, J. W. Jonker, *Adv. Drug Delivery Rev.* **2003**, *55*, 3–29.
[3] S. Shukla, C. Schwartz, K. Kapoor, A. Kouanda, S. V. Ambudkar, *Drug Metab. Dispos.* **2012**, *40*, 304–312.
[4] S. V. Ambudkar, I. Kim, Z. E. Sauna, *Eur. J. Pharm. Sci.* **2006**, *27*, 392–400.
[5] S. G. Aller, J. Yu, A. Ward, Y. Weng, S. Chittaboina, R. Zhuo, P. M. Harrell, Y. T. Trinh, Q. Zhang, I. L. Urbatsch, G. Chang, *Science* **2009**, *323*, 1718–1722.
[6] S. Dey, M. Ramachandra, I. Pastan, M. M. Gottesman, S. V. Ambudkar, *Proc. Natl. Acad. Sci. USA* **1997**, *94*, 10594–10599.
[7] T. W. Loo, M. C. Bartlett, D. M. Clarke, *J. Biol. Chem.* **2003**, *278*, 39706–39710.
[8] M. R. Lugo, F. J. Sharom, *Biochemistry* **2005**, *44*, 14020–14029.
[9] S. Orlowski, L. M. Mir, J. Belehradek Jr, M. Garrigos, *Biochem. J.* **1996**, *317*, 515–522.
[10] C. F. Higgins, *Nature* **2007**, *446*, 749–757.
[11] K. Kapoor, H. Sim, S. V. Ambudkar in *Resistance to Targeted Anti-Cancer Therapeutics, Vol. 1* (Ed.: B. Bonavida), Springer, New York, **2013**, pp. 1–34.
[12] I. Sekine, C. Shimizu, K. Nishio, N. Saijo, T. Tamura, *Int. J. Clin. Oncol.* **2009**, *14*, 112–119.
[13] Z. Shi, A. K. Tiwari, S. Shukla, R. W. Robey, S. Singh, I. W. Kim, S. E. Bates, X. Peng, I. Abraham, S. V. Ambudkar, T. T. Talele, L. W. Fu, Z. S. Chen, *Cancer Res.* **2011**, *71*, 3029–3041.
[14] S. Shukla, C. P. Wu, S. V. Ambudkar, *Expert Opin. Drug Metab. Toxicol.* **2008**, *4*, 205–223.
[15] H. Tao, Y. Weng, R. Zhuo, G. Chang, I. L. Urbatsch, Q. Zhang, *ChemBioChem* **2011**, *12*, 868–873.
[16] D. Boesch, C. Gavériaux, B. Jachez, A. Pourtier-Manzanedo, P. Bollinger, F. Loor, *Cancer Res.* **1991**, *51*, 4226–4233.
[17] F. Loor, *Expert Opin. Invest. Drugs* **1999**, *8*, 807–835.
[18] M. C. Bagley, J. W. Dale, E. A. Merritt, X. Xiong, *Chem. Rev.* **2005**, *105*, 685–714.
[19] A. Bertram, J. S. Hannam, K. A. Jolliffe, F. González-López de Turiso, G. Pattenden, *Synlett* **1999**, 1723–1726.
[20] A. Bertram, A. J. Blake, F. González-López de Turiso, J. S. Hannam, K. A. Jolliffe, G. Pattenden, M. Skae, *Tetrahedron* **2003**, *59*, 6979–6990.
[21] E. A. Merritt, M. C. Bagley, *Synthesis* **2007**, 3535–3541.
[22] M. W. Bredenkamp, C. W. Holzapfel, W. J. van Zyl, *Synth. Commun.* **1990**, *20*, 2235–2249.
[23] E. Aguilar, A. I. Meyers, *Tetrahedron Lett.* **1994**, *35*, 2473–2476.
[24] C. D. J. Boden, G. Pattenden, T. Ye, *Synlett* **1995**, 417–419.
[25] C. Moody, M. Bagley, *J. Chem. Soc. Perkin Trans. 1* **1998**, 601–608.
[26] P. S. Ramamoorthy, J. Gervay, *J. Org. Chem.* **1997**, *62*, 7801–7805.
[27] D. Hudson, *J. Org. Chem.* **1988**, *53*, 617–624.
[28] A. J. Blake, J. S. Hannam, K. A. Jolliffe, G. Pattenden, *Synlett* **2000**, 1515–1518.
[29] C. Martin, G. Berridge, P. Mistry, C. Higgins, P. Charlton, R. Callaghan, *Br. J. Pharmacol.* **1999**, *128*, 403–411.
[30] P. Mistry, A. J. Stewart, W. Dangerfield, S. Okiji, C. Liddle, D. Bootle, J. A. Plumb, D. Templeton, P. Charlton, *Cancer Res.* **2001**, *61*, 749–758.
[31] E. Fox, S. E. Bates, *Expert Rev. Anticancer Ther.* **2007**, *7*, 447–459.
[32] W. Priebe, N. T. Van, T. G. Burke, R. Perez-Soler, *Anticancer Drugs* **1993**, *4*, 37–48.
[33] B. Sarkadi, E. M. Price, R. C. Boucher, U. A. Germann, G. A. Scarborough, *J. Biol. Chem.* **1992**, *267*, 4854–4858.
[34] S. V. Ambudkar, I. H. Lelong, J. Zhang, C. O. Cardarelli, M. M. Gottesman, I. Pastan, *Proc. Natl. Acad. Sci. USA* **1992**, *89*, 8472–8476.
[35] H. Omote, M. K. Al-Shawi, *J. Biol. Chem.* **2002**, *277*, 45688–45694.
[36] A. K. Tiwari, K. Sodani, C. L. Dai, A. H. Abuznait, S. Singh, Z. J. Xiao, A. Patel, T. T. Talele, L. Fu, A. Kaddoumi, J. M. Gallo, Z. S. Chen, *Cancer Lett.* **2013**, *328*, 307–317.
[37] G. Klopman, L. M. Shi, A. Ramu, *Mol. Pharmacol.* **1997**, *52*, 323–334.
[38] P. Crivori, B. Reinach, D. Pezzetta, I. Poggesi, *Mol. Pharm.* **2006**, *3*, 33–44.
[39] I. K. Pajeva, C. Globisch, M. Wiese, *ChemMedChem* **2009**, *4*, 1883–1896.
[40] T. W. Loo, D. M. Clarke, *J. Biol. Chem.* **2001**, *276*, 14972–14979.
[41] F. Tiberghien, F. Loor, *Anticancer Drugs* **1996**, *7*, 568–578.
[42] R. W. Robey, K. Steadman, O. Polgar, K. Morisaki, M. Blayney, P. Mistry, S. E. Bates, *Cancer Res.* **2004**, *64*, 1242–1246.
[43] S. Shukla, R. W. Robey, S. E. Bates, S. V. Ambudkar, *Drug Metab. Dispos.* **2009**, *37*, 359–365.
[44] S. V. Ambudkar, *Methods Enzymol.* **1998**, *292*, 504–514.
[45] Z. E. Sauna, S. V. Ambudkar, *Proc. Natl. Acad. Sci. USA* **2000**, *97*, 2515–2520.

Received: August 30, 2013
Published online on November 29, 2013